

Articles

Semiconducting Organometallics: Electrical Conducting Behavior of $\text{Fe}(\text{CO})_3(\text{diene})$ Doped with Iodine and Their ^{57}Fe Mössbauer Spectroscopic Studies

Seiichi Miyanaga,[†] Hajime Yasuda,^{*†} Hiroshi Sakai,[†] and Akira Nakamura[†]

Department of Macromolecular Science, Faculty of Science, Osaka University, Toyonaka, Osaka 560, Japan, and Research Reactor Institute, Kyoto University, Kumatori, Sennan-gun, Osaka 590-04, Japan

Received July 29, 1988

The measurement of electrical conductivity of a series of air-stable transition-metal organometallics has been performed in vacuo after doping with appropriate amounts of iodine. A variety of diene, triene, and polyene complexes of $\text{Fe}(\text{CO})_3$ as well as substituted ferrocenes, $\text{Cr}(\text{CO})_3(\text{arene})$, $\text{CoCp}(\text{C}_4\text{Ph}_4)$, and Cp_2MoX_2 were found to behave as good semiconductors ($\sigma > 10^{-6} \text{ S cm}^{-1}$) when pressed samples are exposed to iodine vapor. Mössbauer, IR, and ^{13}C CPMAS NMR studies on the iodine-doped $\text{Fe}(\text{CO})_3(\text{diene})$ complexes reveal the generation of a low-spin $\text{Fe}(\text{II})$ species, i.e., $\text{FeI}_2(\text{CO})_2(\text{diene})$, as a major product, that acts as a key substance to construct the carrier transport system. The addition of excess iodine finally leads to the formation of electrically nonconducting FeI_2 .

Introduction

Recent accelerated development in the chemistry of electrically conducting materials in both inorganic (e.g. $\text{YBa}_2\text{Cu}_3\text{O}_x$) and organic fields (e.g., tetracyanoquinodimethane-tetrathiafulvalene (TCNQ-TTF) type salts, doped polyacetylene, etc.) prompted us to survey the electrical nature of organometallics to find new types of conducting systems since these can be viewed as hybrids between organic and inorganic components. If organometallic systems composed of metal, organic ligand, and a donor or an acceptor can represent a suitable device for controlling lattice architecture, electronic delocalization in low-dimensional multimolecular array, and chemical reactions that generate a carrier transport sequence, these materials may show unique conducting behavior. On the basis of this assumption, we have explored the measurement of electrical conductivity for a wide variety of organotransition-metal complexes before and after doping with iodine (a typical dopant) to collect fundamental aspects on their conducting behavior. Although a variety of synthetic methods has already been sufficiently accumulated for air-stable organometallics, the whole picture of their conducting behavior has surprisingly not yet been well documented except the following systems: donor-acceptor or charge-transfer complexes containing metallocenes,¹⁻⁵ $\text{IrCl}_2(\text{CO})_2$,⁶ $\text{Nb}_3\text{Cl}_3(\text{C}_6\text{Me}_6)_3$,⁷ MeSnCl_3 ,⁸ and organometallic polymers⁹⁻¹⁶ involving Krogmann¹⁴ and Magnus salts.^{15,16} As a related system, doped metal porphyrins,^{17,18} metal phthalocyanines,¹⁹⁻²¹ and metal thiolates²² are reported to exhibit fairly good conductivities. This paper describes general aspects of the conducting properties of the transition-metal organometallics and focuses in particular on the behavior of $\text{Fe}(\text{CO})_3(\text{diene})$ as a function of incremental partial oxidation with iodine.

Results and Discussion

General Aspects on the Conducting Property of Organometallics. Almost all organometallic precursors

- (1) Melby, L. R.; Harder, R. J.; Hertler, W. R.; Mahler, W.; Benson, R. E.; Mochel, W. E. *J. Am. Chem. Soc.* **1962**, *84*, 3374.
- (2) Iijima, S.; Tanaka, Y. *J. Organomet. Chem.* **1984**, *270*, C11.
- (3) Mueller-Westerhoff, U. T.; Eilbracht, P. *J. Am. Chem. Soc.* **1972**, *94*, 9272.
- (4) Pittman, Jr., C. V.; Sasaki, Y.; Mukherjee, T. K. *Chem. Lett.* **1975**, 383.
- (5) Cowan, D. O.; LeVande, C. *J. Chem. Soc.* **1972**, *94*, 9271.
- (6) Ginsberg, A. P.; Koepke, J. W.; Hauser, J. J.; West, K. W.; Disalvo, E. J.; Sprinkle, C. R.; Cohen, R. L. *Inorg. Chem.* **1976**, *15*, 514.
- (7) Goldberg, S. Z.; Spivack, B.; Stanley, G.; Eisenberg, R.; Braitsch, D. M.; Miller, J. S.; Abkowitz, M. *J. Am. Chem. Soc.* **1977**, *99*, 110.
- (8) Matsubayashi, G.; Ueyama, K.; Tanaka, T. *J. Chem. Soc., Dalton Trans.* **1985**, 465.
- (9) Cowan, D. O.; Park, J.; Pittman, Jr., C. U.; Sasaki, Y.; Mukherjee, T. K.; Diamond, N. A. *J. Am. Chem. Soc.* **1972**, *94*, 5110.
- (10) Pittman, Jr., C. U.; Suryanarayanan, B. *J. Am. Chem. Soc.* **1974**, *96*, 7916.
- (11) Sanechika, K.; Yamamoto, T.; Yamamoto, A. *Polym. J.*, **1981**, *13*, 255.
- (12) Yasuda, H.; Miyanaga, S.; Nakamura, A. *Macromolecules* **1984**, *17*, 2453.
- (13) Yasuda, H.; Noda, I.; Morita, Y.; Nakamura, H.; Miyanaga, S.; Nakamura, A. *Metal-Containing Polymeric Systems*; Carraher, Jr., C. E., Pittman, Jr., C. V., Sheats, J. E., Eds.; Plenum: New York, 1985; p 275.
- (14) Zeller, H. R. *J. Phys. Chem. Solids* **1974**, *35*, 77.
- (15) Lecrone, F. N.; Minot, M. J.; Perlstein, J. H. *Inorg. Nucl. Chem. Lett.* **1972**, *8*, 173.
- (16) Tsujikawa, I.; Kubota, R.; Enoki, T.; Miyajima, S.; Kobayashi, H. *J. Phys. Soc. Jpn.* **1977**, *43*, 1459.
- (17) Hoffman, B. M.; Ibers, J. A., *Acc. Chem. Res.* **1983**, *16*, 15.
- (18) Phillips, T. E.; Scaringe, R. P.; Hoffman, B. M.; Ibers, J. A. *J. Am. Chem. Soc.* **1980**, *102*, 3435.
- (19) Diel, B. N.; Inabe, T.; Lyding, J. W.; Schoch, Jr., K. F.; Kannewurf, C. R.; Marks, T. J. *J. Am. Chem. Soc.* **1983**, *105*, 1551.
- (20) Metz, J.; Hanack, M. *J. Am. Chem. Soc.* **1983**, *105*, 828.
- (21) Diel, B. N.; Inabe, T.; Jaggi, N. K.; Lyding, J. W.; Schneider, O.; Hanack, M.; Kannewurf, C. R.; Marks, T. J.; Schwartz, L. H. *J. Am. Chem. Soc.* **1984**, *106*, 3207.
- (22) Cassoux, P.; Valade, L.; Vogt, T.; Vincente, R.; Ribas, J.; Kahn, O.; Thuery, P. *Synth. Met.* **1987**, *19*, 573.

[†] Osaka University.

[‡] Kyoto University.

Table I. Electrical Conductivity of Organometallics at 20 °C after Doping with Iodine (the Uptake That Shows the Maximum Conductivity in Parentheses)


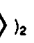

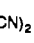

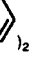
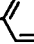
groups	precursor complex	σ , S cm ⁻¹	I ₂ /metal ^b	
1 ($\sigma < 10^{-6}$ S cm ⁻¹)	Fe(CO) ₃ (1,4-diphenyl-1,3-butadiene)	2 × 10 ⁻⁵	0.03	
	Fe(CO) ₃ (1,6-diphenyl-1,3,5-hexatriene)	5 × 10 ⁻⁵	0.03	
	Fe(CO) ₃ (1,8-diphenyl-1,3,5,7-octatetraene)	6 × 10 ⁻⁵	0.03	
	Fe(CO) ₃ (bicyclo-1,3-octadienyl)	3 × 10 ⁻⁵	0.05	
	Fe(CO) ₃ (β -carotene)	8 × 10 ⁻⁶	0.03	
	[Fe(CO) ₃] ₂ (1,3,5,7-decatetraene)	5 × 10 ⁻⁵	0.05	
	[Fe(CO) ₃] ₂ (η^3, η^3 -2,8-decadien-1,10-yl)	4 × 10 ⁻⁵	0.04	
	[Fe(CO) ₄ (η^3 -methylallyl)] ⁺ [BF ₄] ⁻	3 × 10 ⁻⁶	0.02	
	FeI ₂ (CO) ₄ , RuI ₂ (CO) ₄	3 × 10 ⁻⁵	0.03	
	CoCp(1,2,3,4-tetraphenylcyclobutadiene)	4 × 10 ⁻⁶	0.09	
	NiClCp(PPh ₃), NiCp ₂	2 × 10 ⁻⁵	0.12	
	Cr(CO) ₃ (η^6 -1,4-diphenyl-1,3-butadiene)	3 × 10 ⁻⁵	0.05	
	2 ($10^{-6} > \sigma > 10^{-10}$)	NiX ₂ (PPh ₃) ₂ (X = Cl, Br)	6 × 10 ⁻⁸	0.04–0.07 ^c
		Ni(CNC ₆ H ₄ CH ₃) ₄	3 × 10 ⁻⁷	0.13
CoX ₂ (PPh ₃) ₂ (X = Cl, Br)		6 × 10 ⁻⁸	0.04–0.06 ^c	
CoI ₂ Cp(PPh ₃)		2 × 10 ⁻⁸	0.06 ^c	
CoCp ₂		2 × 10 ⁻⁷	0.07–0.09	
[Fe(CO) ₂ Cp] ₂		7 × 10 ⁻⁸	0.05	
FeClCp(CO) ₂		7 × 10 ⁻⁸	0.01 ^c	
FeICp(CO) ₂		7 × 10 ⁻⁹	0.01 ^c	
FeBr(CO) ₃ (η^3 -allyl)		2 × 10 ⁻⁹	0.02 ^c	
[Ru(CO) ₃] ₂ (1,4-diphenylbutadiene) ₃		6 × 10 ⁻⁸	0.08	
RuCp ₂		2 × 10 ⁻⁷	0.08	
Cr(CO) ₅ (PPh ₃)		3 × 10 ⁻⁸	0.07	
[MoCp(CO) ₃] ₂		6 × 10 ⁻⁹	0.01	
W(CO) ₅ (PPh ₃)		2 × 10 ⁻⁷	0.16	
3 ($\sigma \leq 10^{-10}$ S cm ⁻¹)	PdCl ₂ (PPh ₃) ₂	2 × 10 ⁻¹⁰	0.01 ^c	
	PdCl ₂ (C ₈ H ₁₂)	<10 ⁻¹²	0.00 ^c	
	[PdCl(C ₈ H ₅) ₂]	<10 ⁻¹²	0.00 ^c	
	PtCl ₂ (PPh ₃) ₂	8 × 10 ⁻¹⁰	0.04 ^c	
	NiBr ₂ [bis(diphenylphosphino)ethane]	7 × 10 ⁻¹⁰	0.03 ^c	
	CoI ₂ (CO)Cp	<10 ⁻¹²	0.00 ^c	
	Co ₂ (CO) ₆ (PhC≡CPh)	<10 ⁻¹²	0.00 ^c	
	Co ₃ (CO) ₉ (CCOOC ₂ H ₅)	5 × 10 ⁻¹⁰	0.01	
	Fe ₂ (CO) ₉	7 × 10 ¹⁰	0.02	
	Ru ₃ (CO) ₁₂	9 × 10 ⁻¹⁰	0.01	
	M(CO) ₆ (M = Cr, Mo, W)	10 ⁻¹²	0.00	
	MCp ₂ Cl ₂ (M = Ti, Zr, Hf)	10 ⁻¹²	0.00	

^a All the organometallics listed are insulators ($\sigma < 10^{-12}$ S cm⁻¹) before doping. Doping was performed on the compressed disks of pure samples. ^b Determined on the basis of the elemental analysis. ^c Calculated from increases in weight, assuming that complexes do not decompose evolving gaseous products.

tested here are environmentally stable and highly purified crystalline compounds that are insulating ($\sigma > 10^{-12}$ S cm⁻¹). The maximum direct-current electrical conductivities for these compounds upon doping with an appropriate amount of iodine are summarized in Table I (results for some metallocene derivatives are given separately in Table II). The doping was performed by diffusion of iodine vapor (0.01–0.5 equiv) onto the compressed circular disks (thickness ca. 0.5 mm, diameter 10 mm) of organometallics at 20 °C in a sealed vessel under reduced pressure, and the measurement of conductivity was carried out in vacuo (10⁻² Torr) by using the conventional two- or four-probe technique at 77–335 K. Handling of the doped samples was performed in argon to avoid the effect of moisture and air on the conductivity. As a result of systematic studies, the complexes tested here can be classified into three groups on the basis of the extent of conductivity.

A series of tricarbonyl(diene)iron complexes and cyclopentadienyl compounds of Co and Ni along with a tricarbonyl(arene)chromium complex were first found to show a fairly good conductivity ($\sigma = 10^{-5}$ – 10^{-6} S cm⁻¹). Thus the direct-current conductivity increases rapidly by 6–8 orders of magnitude upon doping of these precursors. Most of these complexes involve a conjugated ligand (Cp or diene), but the extension of the conjugation system from diene to triene, tetraene, and polyenes (e.g., β -carotene) did not affect largely the conductivity as opposed to our expectation as observed in case of the Fe(CO)₃(diene)

Table II. Electrical Conductivity of Iodine-Doped Substituted Ferrocenes^a

complex	σ , S cm ⁻¹	I ₂ /Fe ratio ^b
ferrocene (Fc)	4.3 × 10 ⁻⁸	0.12
Fc(CH ₂ - ) ₂	2.1 × 10 ⁻⁶	0.09
Fc(CH ₂ CH ₂ - ) ₂	3.0 × 10 ⁻⁴	0.11
Fc(CH ₂ CH ₂ CH ₂ - ) ₂	4 × 10 ⁻⁴	0.13
Fc(CH ₂ -  -CN) ₂	1.7 × 10 ⁻⁴	0.10
Fc(CH ₂ - ) ₂	2.7 × 10 ⁻⁵	0.09
Fc(CH ₂ - ) ₂	1.0 × 10 ⁻⁴	0.12
Fc(CH ₂ - ) ₂	1.1 × 10 ⁻⁵	0.08

^a Iodine doping was conducted onto the compressed disks at 20 °C in vacuo. ^b Determined on the basis of the elemental analysis.

family. This behavior differs greatly from the general trend that the highly conjugated organic systems such as

doped polyacetylenes and polyaromatics (e.g., perylene) induce higher conductivity by extending the conjugation. More remarkable is that the present system requires only a minute amount of dopant ($I_2/M < 0.05$ mol/mol) before reaching the critical point (the point that shows the maximum conductivity). In every case, the color of precursor complexes turns brown-black by partial oxidation with iodine vapor not only on the surface but also throughout the volume of the sample.

In sharp contrast to the above complexes, doped samples of various metal carbonyl compounds like $Fe_2(CO)_9$ and $Ru_3(CO)_{12}$ along with group 4A metallocene dihalides ($M = Ti, Zr, Hf$) and group 8 metal halides ligated by phosphine(s), cyclo-1,5-octadiene, or allyl(s) are all insulators irrespective of the formal oxidation number of the metal center. This class of complexes took on no significant coloration during the doping and could be recovered without any chemical change. Thus, the iodine doping brings about no oxidation in case of the group 3 organometallics listed in Table I.

Although $[Fe(CO)_2Cp]_2$, $FeX(CO)_2Cp$ ($X = Cl, Br, I$), and $[Mo(CO)_3Cp]_2$, which belong in group 2, contain both CO and Cp ligands in a molecule, these complexes show remarkably lower conductivity ($\sigma = 10^{-7}$ – 10^{-10} S cm^{-1}) as compared with the group 1 complexes irrespective of the dopant concentration. Other organometallics belonging in this category are metal carbonyl phosphine ($M = Cr, W$), metal halide phosphine complexes ($M = Ni, Co$), and nickel isonitrile complexes.

Sandwich-type metallocenes are typical organometallics that have been studied most extensively for their electrical properties. These include donor (e.g., TCNQ) and acceptor (e.g., TTF, I_3^-) complexes of ferrocene,^{1,2} mixed-valency ferrocenylene,³⁻⁵ cobaltocene,¹ bicobaltocene,²³ and their polymer derivatives.⁹⁻¹¹ The X-ray crystal structure of undoped ferrocene²⁴⁻²⁶ revealed that the Cp-Fe-Cp axis of each molecule is oriented perpendicular to that of the neighboring ferrocene while its I_3^- , Br_3^- , and TCNQ salts force the Cp-Fe-Cp axes to orient parallel to each other, resulting in the formation of ferrocene layers.^{27,28} If the formation of a ferrocene stack or column is requisite to construct the carrier transport system, introduction of rather long chains into the Cp ring is expected to affect the conductivity, because the molecules may be aligned so as to produce a linear or planar multimolecular array as a consequence of the steric as well as hydrophobic or electrostatic interactions of the substituents. The principle is the same as that accepted in the chemistry of liquid crystals. On the basis of this assumption, we have prepared several substituted ferrocenes and examined their conductivity after doping. As a result, an increase in conductivity was indeed observed in some favorable cases (Table II). $Fc(CH_2CH_2C_6H_5)_2$ and $Fc(CH_2\beta-C_{10}H_7)_2$ show a reversible oxidation wave in cyclic voltammetry at $E_{1/2} = 0.38$ and 0.42 V, respectively, somewhat smaller potentials as compared with that of ferrocene ($E_{1/2} = 0.48$ V versus SCE). Thus several substituted ferrocenes are more easily oxidized than the parent ferrocene molecule due to the electronic effect and presumably due to a difference in the mode of molecular packing.

Table III. Conductivity of the Wedged Metallocene Compounds of Mo and W after Doping with Iodine^a

precursor complex	σ , S cm^{-1}	$I_2/metal^b$
Cp_2MoH_2	1.0×10^{-6}	0.12
Cp_2MoCl_2	1.9×10^{-5}	0.08
Cp_2MoBr_2	5.7×10^{-4}	0.09
$Cp_2Mo(PhC\equiv CPh)$	1.0×10^{-7}	0.08
Cp_2WH_2	4.7×10^{-7}	0.10
Cp_2WCl_2	1.5×10^{-7}	0.09
Cp_2WBr_2	3.0×10^{-6}	0.07
$Cp_2W(PhC\equiv CPh)$	6.1×10^{-7}	0.03

^aDoping was conducted onto the compressed disks at 20 °C.

^bCalculated from increase in weight of samples by doping, assuming that complexes do not evolve gaseous products.

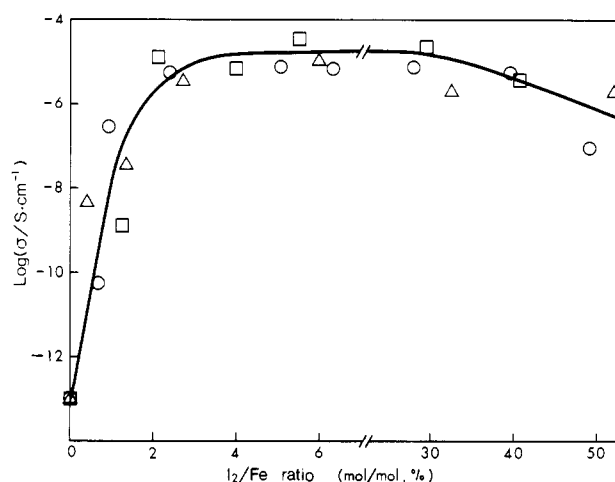


Figure 1. Direct-current conductivity vs iodine uptake plots for $Fe(CO)_3(1,4$ -diphenylbutadiene) (1, ○), $Fe(CO)_3(1,6$ -diphenylhexatriene) (2, Δ), and $Fe(CO)_3(1,8$ -diphenyloctatetraene) (3, □).

Is the parallel sandwich-type metallocene structure really required for the present type of conducting system? To answer this question, we have measured the conductivity of various wedged metallocenes after doping. As opposed to our expectation, group 6 transition-metal metallocene compounds MCp_2X_2 ($X = H, Cl, Br$) function as a fairly good semiconductors, although $MoCp_2(PhC\equiv CPh)$ (10^{-7} S cm^{-1}) and $WCp_2(PhC\equiv CPh)$ (10^{-8} S cm^{-1}) exhibit relatively low conductivity. The molybdenum family usually shows higher conductivity as compared with the corresponding tungsten derivatives (Table III).

Thus it is obvious from the present work that a variety of air-stable low-valent organometallics of group 6–8 elements can readily be converted into semiconductors by partial oxidation with iodine. The conductivity is almost independent of the metallocene structures, parallel sandwich or wedged. On the other hand, a majority of high-valent metal complexes together with some low-valent complexes with high oxidation potentials do not act as semiconductors.

Conducting Behavior of $Fe(CO)_3$ (diene) after Doping. To gain an insight into the conducting mechanism, the chemical change during the solid-state doping was investigated on the basis of chemical characterization and spectral studies using several $Fe(CO)_3$ (diene) complexes as a typical organometallic precursor. Figure 1 shows the direct-current conductivity of polycrystalline iron complexes $Fe(CO)_3(1,4$ -diphenylbutadiene) (1), $Fe(CO)_3(1,6$ -diphenylhexatriene) (2), and $Fe(CO)_3(1,8$ -diphenyloctatetraene) (3) as a function of dopant concentration. The uptake of iodine and the I_2/Fe ratio were determined on the basis of the calibration curve obtained from the elemental analysis of iodine and Fe in the doped samples

(23) Lau, C.; Singh, P.; Cline, S. J.; Seiders, R.; Brookhart, M.; Marsh, W. E.; Hodgson, D. J.; Hatfield, W. E. *Inorg. Chem.* **1982**, *21*, 208.

(24) Takusagawa, F.; Koetzle, T. F. *Acta Crystallogr.* **1979**, *B35*, 1074.

(25) Seiler, P.; Dunitz, J. D. *Acta Crystallogr.* **1979**, *B35*, 1068.

(26) Freyberg, D. P.; Robbins, J. L.; Raymond, K. N.; Smart, J. C. *J. Am. Chem. Soc.* **1979**, *101*, 892.

(27) Bernstein, T.; Herstein, F. H. *Acta Crystallogr.* **1968**, *B24*, 1640.

(28) Bats, J. W.; de Boer, J. J.; Bright, D. *Inorg. Chim. Acta* **1971**, *5*, 605.

Table IV. Mössbauer Parameters for Fe(CO)₃(diene) before and after Iodine Doping^a

complex	undoped samples		doped samples				
	QS, mm/s	IS, mm/s	QS, mm/s	IS, mm/s	species	A/B/C ratio	I ₂ /Fe ^b
Fe(CO) ₃ (1,4-DB) (1)	1.621	0.067	0.455	0.196	B	74/26/0	0.25
Fe(CO) ₃ (1,6-DH) (2)	1.628	0.080	0.429	0.137	B	62/38/0	0.37
Fe(CO) ₃ (1,8-DO) (3)	1.685	0.063			B	62/35/0	0.32
Fe(CO) ₃ (BCO) (4)	1.428	0.021			B	82/2/6	0.16
			2.890	1.360	C		
Fe(CO) ₃ (butadiene) ^c	1.46	0.027					
Fe(CO) ₃ (PB) ^c	1.59	0.047					
FeI ₂ (CO) ₄			0.305	0.063			

^aSpectra were measured at -195 °C. 1,4-DB, 1,4-diphenyl-1,3-butadiene; 1,6-DH, 1,6-diphenyl-1,3,5-hexatriene; 1,8-DO, 1,8-diphenyl-1,3,5,7-octatriene; BCO, bicyclo-1,3-octadienyl; PB, 1-phenyl-1,3-butadiene. ^bDetermined by elemental analysis. ^cSee ref 37.

synthesized separately under the same conditions. Especially noteworthy is that the conductivity increases rapidly by 6–7 orders of magnitude up to 10⁻⁵ S cm⁻¹ by the addition of only a small amount of iodine before leveling off at around 0.03 mol/mol of I₂/Fe ratio. CoCp(1,2,3,4-tetraphenylcyclobutadiene) and CoCp(2,3,4,5-tetraphenyl-2,4-pentadien-1-one) also showed similar behavior (I₂/Co ratio at the critical point ca. 0.1 mol/mol). The whole picture of the conducting behavior compares closely with that observed for the polyacetylene system, which requires only 0.02 equiv of AsF₅ per CH unit at the critical point.²⁹ In this regard, the present system differs greatly from the [FeCp₂][I_n] (n = 1–6) family, which requires a stoichiometric or excess amount of iodine to construct the complex.³⁰ The variable-temperature measure of the doped Fe(CO)₃(diene) confirms that these materials belong to the intrinsic semiconductors (the conductivity increases with increasing temperature). The activation energies (ΔE) for semiconduction calculated for 1, Fe(CO)₃(bicycloocta-1,3-dienyl) (4), and Cr(CO)₃(η⁶-1,4-diphenylbutadiene) are 0.32, 0.73, and 0.63 eV, respectively, in the range 240–315 K. These are nearly comparable to those reported for semiconducting materials like poly(vinylferrocene)/ClO₄ (0.37–0.43 eV),³¹ Sn(phthalocyanine)/I_{5.5} (0.68 eV),³² and polyaromatics/I_n (0.1–0.3 eV).³³ The Seebeck coefficient of iodine-doped sample of 1 is found to be positive over the whole measurement range (I₂/Fe = 0.01, 60 μV/K; I₂/Fe = 0.04–0.08, 15–22 μV/K). Thus the majority carriers are holes. The observed Seebeck coefficient is rather small and hence hampered determinations of effective mass and the mobility of the hole.

Mössbauer Spectroscopic Studies on the Fe(CO)₃(diene) System. ⁵⁷Fe Mössbauer spectroscopic techniques have been applied to the compressed disks of 1–4 at 77 K before and after iodine doping to elucidate the mode of the solid-state reaction. The precursor Fe(0) complexes (1–4) show a doublet peak (A) due to the quadrupole splitting (QS), whose values are nearly comparable with those for simple Fe(CO)₃(butadiene) as summarized in Table IV (see Figure 2a, for example). A slight increase in QS is observed when the conjugation of the ligand is extended. Sublimation of iodine onto the compressed disks of 1–3 in a range I₂/Fe < 0.3 mol/mol brings about a new peak designated as B (see Figure 2b). The QS and IS (isomer shift) values for this species are in line with those for hexacoordinating low-spin Fe(II) species such as *cis*-

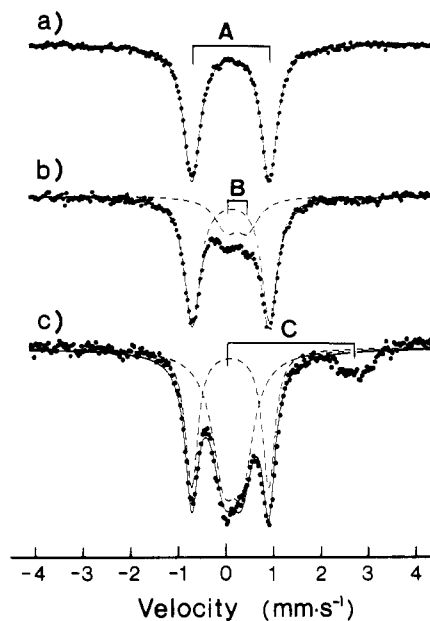


Figure 2. Mössbauer spectra of Fe(CO)₃(1,4-diphenylbutadiene) before and after iodine doping: (a) undoped, (b) doped, I₂/Fe = 0.24, (c) doped, I₂/Fe = 0.51.

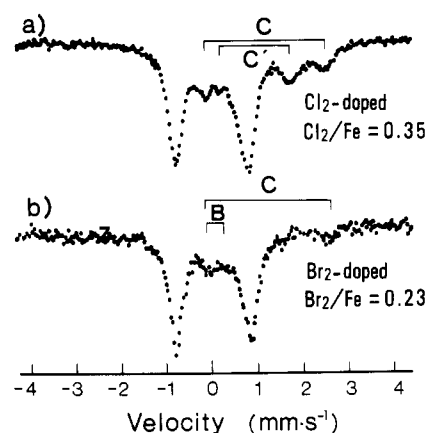


Figure 3. Mössbauer spectra of Fe(CO)₃(1,4-diphenylbutadiene) doped with chlorine and bromine.

FeI₂(CO)₄ (QS, 0.32; IS, 0.06), *cis*-FeCl₂(CO)₄ (QS, 0.26; IS, 0.05), FeI₂(CO)₂(PPh₂Et)₂ (QS, 0.37; IS, 0.11), and FeI₂(CO)₃(PPh₃) (QS, 0.44; IS, 0.07),^{34–36} but these values differ greatly from those for a vast majority of Fe(0), Fe(I), high-spin Fe(II), and high-spin Fe(III) species.^{36–38} Thus,

(29) Chiang, C. K.; Gaw, S. C.; Fincher, Jr., C. R.; Park, Y. W.; McDiarmid, A. G.; Heeger, A. J. *Appl. Phys. Lett.* 1978, 33, 18.

(30) Nesmeyanov, A. N.; Paravahova, E. G.; Nesmeyanova, N. *Dokl. Akad. Nauk SSSR* 1955, 100, 1099.

(31) Shirota, Y.; Kakuta, T.; Mikawa, H. *Macromol. Chem., Rapid Commun.* 1984, 5, 337.

(32) Dirk, C. W.; Mintz, E. A.; Schoch, Jr., K. F.; Marks, T. J. *J. Macromol. Sci., Chem., Educ.* 1981, A16, 275.

(33) For a typical example, see: Dix, G. *Phys. Status Solidi* 1974, A24, 139.

(34) Vasudev, P.; Jones, C. H. W. *Can. J. Chem.* 1973, 51, 405.

(35) Bancroft, G. M.; Libbey, E. T. *J. Chem. Soc., Dalton Trans* 1973, 2103.

(36) Greenwood, N. N.; Gibb, T. C. *Mössbauer Spectroscopy*; Chapman and Hall: London, 1971.

(37) Poskozim, P. S. *J. Inorg. Nucl. Chem.* 1975, 37, 2344.

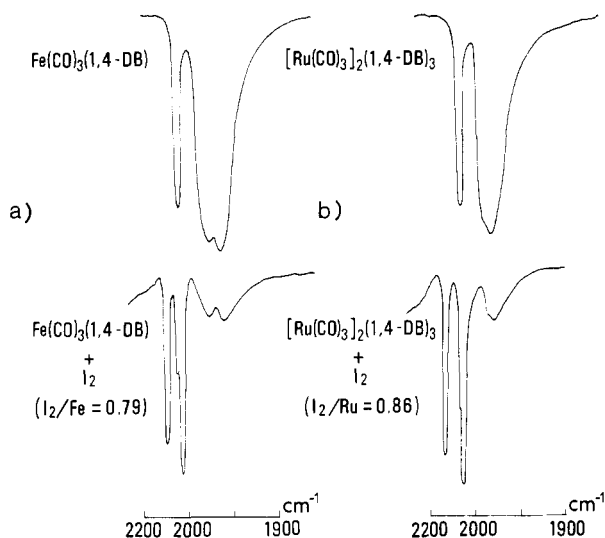


Figure 4. Infrared spectral change of $\text{Fe}(\text{CO})_3(1,4\text{-diphenylbutadiene})$ (a) and $[\text{Ru}(\text{CO})_3]_2(1,4\text{-diphenylbutadiene})_3$ (b) after doping with iodine.

we can readily assign the component (B) as the signal of *cis*- $\text{FeI}_2(\text{CO})_2(\text{diene})$ species. The IR spectral studies also support this structure (vide infra). The cyclic voltammogram of 1 in dimethylformamide (DMF) showed a weak irreversible redox peak at $E_{\text{pa}} = 0.47$ V, while strong second and third oxidation peaks were observed at $E_{\text{pa}} = 0.87$ and 1.25 V vs SCE, respectively, in support of the ready formation of $\text{FeI}_2(\text{CO})_2(\text{diene})$ species (two-electron oxidation).

Another new peak designated as C appears when a relatively large amount of dopant ($\text{I}_2/\text{Fe} > 0.4$ mol/mol) was charged onto the compressed disks as shown in Figure 2c. The doublet (C) is easily assigned to the signal of FeI_2 with reference to the literature.³⁹ This type of oxidation reaction was more pronounced when $\text{Fe}(\text{CO})_3(\text{bicyclo-octa-1,3-dienyl})$ (4) was used (its spectral pattern is very close to that of bromine-doped sample of 1; see Figure 3). The treatment of 1 with Cl_2 and Br_2 vapor in place of I_2 resulted in the predominant formation of FeCl_2 and FeBr_2 (species C) accompanied by the formation of species B as a minor product. Surprisingly the chlorine- and bromine-doped black samples ($\text{X}_2/\text{Fe} = \text{ca. } 0.05$ mol/mol) of 1 ($\sigma = (5\text{--}6) \times 10^{-6}$ S cm^{-1}) show nearly the same conductivity as that for I_2 -doped sample. Since mixing of 1-4 with 0.2-1.0 equiv of FeCl_2 in solution or in the powdered form did not cause any increase in conductivity, the minor component $\text{FeX}_2(\text{CO})_2(\text{diene})$ is expected to function as the key substance to bring about the hole conduction.

A great effort in isolating the $\text{FeX}_2(\text{CO})_2(\text{diene})$ species has failed because these species decompose rapidly to a mixture of FeX_2 , diene, and a small amount of insoluble black mass by dissolving the doped samples in benzene or CH_2Cl_2 at 0-30 °C.

IR and ^{13}C CPMAS NMR Spectral Studies on the Doped $\text{Fe}(\text{CO})_3(\text{diene})$. The IR spectrum (KBr) of $\text{Fe}(\text{CO})_3(1,4\text{-diphenylbutadiene})$ (1) shows the CO stretching vibration at 2042, 1973, and 1960 cm^{-1} , the typical spectral pattern accepted for the $\text{L}_2\text{Fe}(\text{CO})_3$ type complexes of C_{3v} symmetry regarding the $\text{Fe}(\text{CO})_3$ moiety. When doping was conducted on the finely powdered samples of 1, new absorptions appeared at 2090 and 2044 cm^{-1} as shown in Figure 4a, which is essentially invariant with dopant con-

centration up to $\text{I}_2/\text{Fe} \approx 0.5$ mol/mol. The observed spectral pattern is ascribable to hexacoordinated $\text{Fe}(\text{C}-\text{O})_2\text{I}_2\text{L}_2$ species and the higher wavelength shift suggests the presence of Fe-I linkage in the resulting molecule. The higher wavelength shift of the CO absorption is quite common for halogen-attached octahedral iron carbonyl compounds such as $\text{FeCl}(\text{CO})_3(\text{allyl})$ (2091, 2013, 1985 cm^{-1}), $\text{FeI}_2(\text{CO})_3\text{PPh}_2\text{Et}$ (2086, 2045, 2030 cm^{-1}), and $\text{FeI}_2(\text{CO})_4$ (2130, 2090, 2075 cm^{-1}),^{35,40,41} Prolonged doping finally leads to complete loss of CO and liberation of 1,4-diphenylbutadiene as shown by the IR spectrum. Thus the iron species turns to FeI_2 by doping with excess iodine. The formation of FeI_3 is however negligible as revealed by the Mössbauer experiment.

A diene complex of ruthenium carbonyl, $[\text{Ru}(\text{CO})_3]_2(1,4\text{-diphenylbutadiene})_3$,⁴² also shows similar IR spectral change on exposure the powdered sample to iodine vapor. Its Ru-CO absorption (2065, 1983, and 1970 cm^{-1}) upon doping changes to 2135 and 2080 cm^{-1} , nearly the same values as those for $\text{RuI}_2(\text{CO})_4$ ⁴³ (2161, 2107, 2096, and 2066 cm^{-1}) as shown in Figure 4b. This fact indicates the formation of $\text{RuI}_2(\text{CO})_2(1,4\text{-diphenylbutadiene})$ species as a result of iodine doping. Noteworthy is that pure $\text{RuI}_2(\text{CO})_4$ or its mixture with $[\text{Ru}(\text{CO})_3]_2(1,4\text{-diphenylbutadiene})_3$ (1:50 ratio) are insulators while doping with a minute amount of iodine ($\text{I}_2/\text{Ru} = 0.02$ mol/mol) resulted in a significant increase in conductivity, reaching 10^{-6} S cm^{-1} . Thus isoelectronic compounds $\text{RuI}_2(\text{CO})_4$ and $\text{FeI}_2(\text{CO})_4$ as well as the presumed molecules $\text{MI}_2(\text{CO})_2(\text{diene})$ ($\text{M} = \text{Fe, Ru}$) show essentially the same behavior. These results indicate that the present system is composed of $\text{MI}_2(\text{CO})_2(\text{diene})$ and a trace amount of I_2 , where iodine is loosely held as $\text{M}(\text{CO})_2(\text{diene})\text{I}_2 \cdots \text{I}-\text{I}$ or $[\text{M}(\text{CO})_2(\text{diene})\text{I}_3]^+[\text{I}]^-$ to construct an extrinsic semiconducting system.

The resonance Raman spectra of doped samples of 1 ($\text{I}_2/\text{Fe} = 0.05, 0.15,$ and 0.3 mol/mol) did not show appreciable absorption ascribable to I_3^- or I_5^- in the region 85-180 cm^{-1} . Such ions are known to absorb generally at around 100-150 cm^{-1} as reported for $[\text{FeCp}_2]^+[\text{I}_3]^-$,⁴⁴ $[(\text{C}_6\text{H}_5)_4\text{As}]^+[\text{I}_3]^-$,⁴⁵ $(\text{CH}_3)_4\text{NI}_n$,⁴⁶ etc. The major spectral change is a higher wavelength shift of the C=C absorption from 1602 to 1645 cm^{-1} as a result of Fe-I bond formation. Judging from the intensity ratio of these absorptions and the dopant concentration, the resulting $\text{FeI}_2(\text{CO})_2(\text{diene})$ species is concluded not to form a stable donor-acceptor type complex or a mixed-valency complex. In support of this prediction, complex 1 ($\text{Fe}(0)$ species) also did not show any spectral change or an increase in conductivity after mixing it with $\text{Fe}(\text{II})$ species such as $\text{FeI}_2(\text{CO})_4$, FeI_2 , or $[\text{Fe}(\text{CO})_2\text{Cp}]_2$ in 3:1-1:3 ratios.

The ^{13}C CPMAS spectra (67.8 MHz) of $\text{Fe}(\text{CO})_3(1,4\text{-diphenylbutadiene})$ (1) before and after doping are given in Figure 5. The solid-state NMR spectra of 1 and 1,4-diphenylbutadiene (Figure 5, parts b and a, respectively) show nearly the same spectral pattern as those in solution (see the Experimental Section). The doping of 1 resulted in the upfield shift of CH signals assigned to C(1) and C(4) and broadening of the diene C(1)-C(4) signals. The signal intensity ratio between the phenyl and diene carbon signals

(40) Murdoch, H. D.; Weiss, E. *Helv. Chim. Acta* 1962, 45, 1927.

(41) Hales, L. A. W.; Irving, R. J. *J. Chem. Soc. A* 1967, 1389.

(42) Gambino, O.; Valle, M.; Aime, S.; Vaglio, G. A. *Inorg. Chim. Acta* 1974, 8, 71.

(43) Johnson, B. F. G.; Jonston, R. D.; Lewis, J. J. *J. Chem. Soc. A* 1969, 792.

(44) Marks, T. J. *U.S. NITS, AD Rep. AD-A049182* 1977.

(45) Runsink, J.; Swen-Walstra, S.; Migchelsen, T. *Acta Crystallogr.* 1972, B28, 1331.

(46) Nour, E. M.; Chen, L. H.; Laane, J. J. *J. Phys. Chem.* 1980, 90, 2841.

(38) Koerner von Gustorf, E. A.; Grevels, F.-W.; Fischler, I. *The Organic Chemistry of Iron*; Academic Press: New York, 1978; Vol. 1.

(39) Pflétshinger, E. *Z. Phys.* 1968, 209, 119.

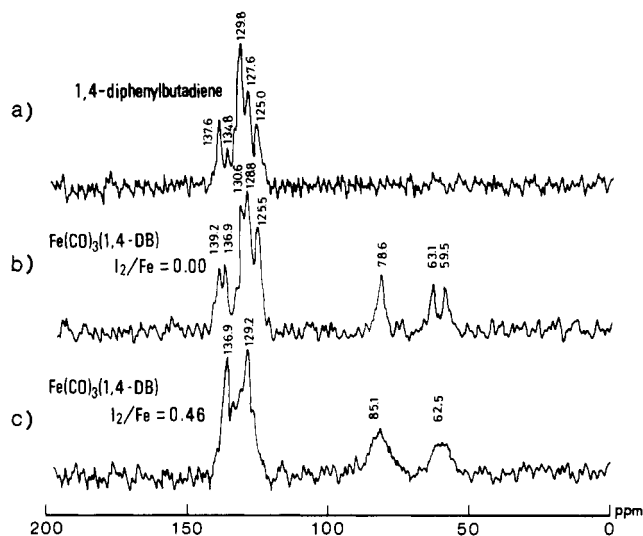


Figure 5. CPMAS ^{13}C NMR spectra of 1,4-diphenylbutadiene, $\text{Fe}(\text{CO})_3(1,4\text{-diphenylbutadiene})$, and the product obtained by doping of $\text{Fe}(\text{CO})_3(1,4\text{-diphenylbutadiene})$.

however remains unchanged. This result supports the formation of $\text{FeI}_2(\text{CO})_2(1,4\text{-diphenylbutadiene})$ species as indicated by the Mössbauer and IR spectroscopic studies. The insufficient resolution of the carbon signals did not enable us to estimate the extent of free 1,4-diphenylbutadiene released from 1 during the doping.

The EPR spectrum of the doped samples of 1–4 ($I_2/\text{Fe} = 0.05, 0.1, \text{ and } 0.3 \text{ mol/mol}$) showed no appreciable signals at 77–298 K. This result at least argues that radical species (neutral radical or π -radical cation) are not generated over the diene ligand during the doping although the radical formation is reported to be largely ligand centered in cases of metallophthalocyanine systems.¹⁹ On the other hand, any reliable information cannot be drawn from this experiment on the oxidation state of resulted iron species because generation of high-spin Fe(II) as well as high-spin Fe(III) species are in many cases undetectable in the EPR spectra (most of these species are normally silent).

The crystal structure of 1 reproduced on the basis of the reported atomic coordinates⁴⁷ is schematically drawn in Figure 6. Complex 4 also exhibits similar molecular packing.⁴⁸ In both cases, there exist double-layered organic stacks composed of ligated dienes in addition to a single layer composed of $\text{Fe}(\text{CO})_3$ fragments. Since the present system requires only a minute amount of dopant ($I_2/\text{Fe} < 0.05 \text{ mol/mol}$) before reaching the critical point, it is reasonable to suggest that the carrier transport takes place without major alternation in their lattice architecture and hence the initial molecular arrangement. Actually a computer simulation of the X-ray diffractions revealed that the addition of iodine to 1 in a ratio of $I_2/\text{Fe} = 0.02\text{--}0.07$ did not affect the spacing of the arrays (i.e., 2θ values assigned to (010), (110), ($\bar{1}\bar{1}\bar{1}$), (201), and (20 $\bar{1}$) reflections). Therefore the electric conduction most likely occurs through the $\text{Fe}(\text{CO})_3$ array in which the $\text{FeI}_2(\text{CO})_2$ moiety exists in an indefinite ratio. In this array, a trace amount of I_2 or I_n^- may be scattered uniformly.

Concluding Remarks

A variety of air-stable organometallic compounds including $\text{Fe}(\text{CO})_3(\text{diene})$ was found to show fairly good

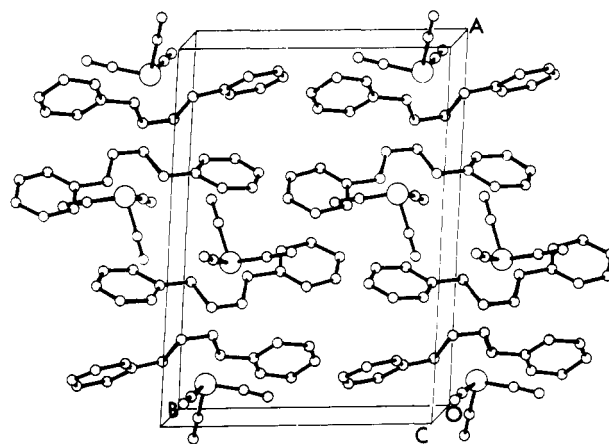


Figure 6. Crystal structure of $\text{Fe}(\text{CO})_3(1,4\text{-diphenylbutadiene})$ reproduced from the atomic coordinates reported in ref 47.

electrical conductivity when iodine doping was conducted on their compressed disks. The major product from $\text{Fe}(\text{CO})_3(\text{diene})$ is $\text{FeI}_2(\text{CO})_2(\text{diene})$, which forms the carrier transport system by interacting with a minute amount of iodine in an inert-gas atmosphere. Charge transport occurs via hole conduction through multimolecular arrays involving $\text{FeI}_2(\text{CO})_2$ moieties. Improvement of the conductivity may be possible when other dopants containing halide groups such as AsF_5 are applied. Furthermore, the use of organometallic polymers enabled us to prepare the semiconducting thin film as communicated earlier.¹² We note that when the doped samples of 1–4 are exposed to air, the conductivity increased instantly up to $10^{-2} \text{ S cm}^{-1}$. This is presumably due to the partial oxidation of the metal species by oxygen (the surface darkens instantly). Further studies are under way to determine the origin of this conductivity enhancement.

Experimental Section

Preparation of Precursor Organometallics. Most of organometallics examined here were prepared according to the known method.^{49,50} Substituted ferrocenes are synthesized by a slight modification of the procedure reported by Jolly,⁵¹ and a series of tricarbonyliron diene in essentially the same manner as described elsewhere.^{48,52}

Electrical Conductivity Measurements. Precursor organometallic samples were divided into a fine powder with a mortar under an argon stream and were compressed into cylindrical pellets of diameter 10 mm and thickness 0.5 mm under pressures of 10–15 tons/cm². The pellet was then fitted to the electrode device by using a carbon-suspended paste (Dotite XC-12, Fujikura Kasei) to connect with Pt wires fitted to electrometers. Iodine doping was conducted in vacuo (10^{-2} Torr) in a glass container joined to a high-vacuum line. The direct-current conductivity was measured by using a standard two- or four-probe technique with a set of a TR8651 potentiometer, a TR6841 ammeter, and a thermometer TR2114 (Takeda Riken) fitted with a chromel-constantan thermocouple in the temperature range 77–335 K. Activation energies (ΔE) were obtained from the slope of $\log \sigma$ vs $1/T$ by using the equation $\sigma/\sigma_0 = \exp(-\Delta E/kT)$ in the range $T = 240\text{--}315 \text{ K}$. Seebeck voltage measurements were run on essentially the same apparatus reported by Matsunaga⁵³ and Chaikin,⁵⁴ using the same pellets as those employed for the electrical conductivity measurement.

(49) Wilkinson, G.; Stone, F. G. A.; Abel, E. W., Eds.; *Comprehensive Organometallic Chemistry*; Pergamon Press: New York, 1973; Vol. 1–11.

(50) Buckingham, J.; Macintyre, J., Eds.; *Dictionary of Organometallic Compounds*; Chapman and Hall: London, 1984; Vol. 1–3.

(51) Jolly, W. L. *Inorg. Synth.* 1968, 11, 120.

(52) Manuel, T. A.; Stafford, S. L.; Stone, F. G. A. *J. Am. Chem. Soc.* 1961, 83, 3597.

(53) Kan, K.; Matsunaga, Y. *Bull. Chem. Soc. Jpn.* 1972, 45, 2096.

(54) Chaikin, P. M.; Kwak, J. F. *Rev. Sci. Instrum.* 1975, 46, 218.

(47) Kuźmina, L. G.; Struchkov, Y. T.; Nekhaev, A. I. *Zh. Strukt. Khim.* 1972, 13, 1115.

(48) Noda, I.; Yasuda, H.; Nakamura, A. *J. Organomet. Chem.* 1983, 250, 447.

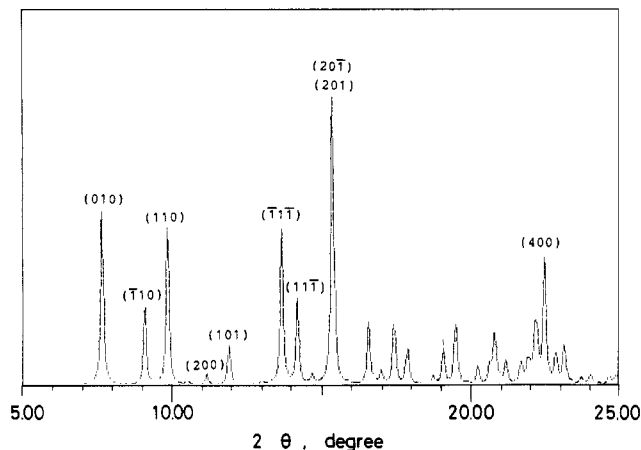


Figure 7. Computer simulation of the powder X-ray diffractions of $\text{Fe}(\text{CO})_3(1,4\text{-diphenylbutadiene})$. The cell parameters used here are $a = 15.884$, $b = 11.581$, $c = 8.404$ Å, $\alpha = 92.48^\circ$, $\beta = 89.79^\circ$, and $\gamma = 96.81^\circ$.

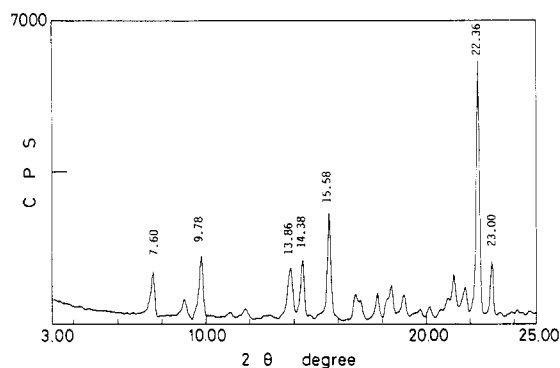


Figure 8. Powder X-ray diffraction pattern of $\text{Fe}(\text{CO})_3(1,4\text{-diphenylbutadiene})$ before iodine doping.

Mössbauer Spectral Measurements. ^{57}Fe Mössbauer spectra were taken in standard transmission geometry at 77 K in vacuo with ^{57}Co in Rh source. The doped samples in the form of compressed disk (diameter 10 mm, thickness 0.1–0.5 mm) were wrapped with aluminum foil to prevent the decomposition on contact with moist air and were mounted in a copper sample holder. The data acquisition was performed with a microcomputer, and the obtained spectra were best fitted with Lorentzian curves. The velocity calibration was made with six peaks of $\alpha\text{-Fe}$.

Solid-State NMR Spectra. ^{13}C CPMAS spectra were run on a JEOL GX-270 spectrometer operating at 67.8 MHz. The

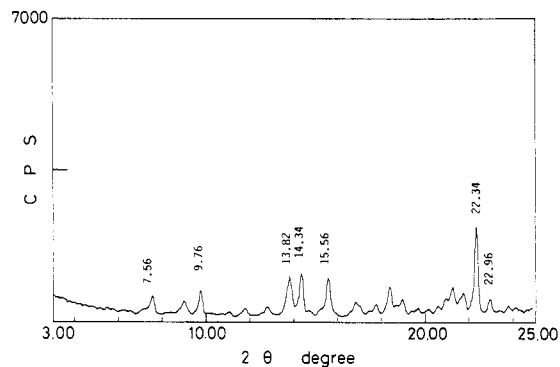


Figure 9. Powder X-ray diffraction pattern of $\text{Fe}(\text{CO})_3(1,4\text{-diphenylbutadiene})$ after iodine doping ($\text{I}_2/\text{Fe} = 0.05$ mol/mol).

powdered samples were packed into a rotor consisting of alumina. Chemical shift values are calibrated with an external adamantane peak, assumed to be 29.5 ppm. The spectra were obtained at 30 °C with MAS spinning rate of 2.5 kHz, contact time of 5.5 ms, and recycle time of 3 s by utilizing the TOSS (total suppression of spinning sidebands) program. The solution ^{13}C NMR (CDCl_3) data are as follows: 1,4-diphenylbutadiene δ 132.8 (C-1 and C-4), 127.5 (C-2 and C-3), 137.4 (C_6H_5), 126.3 (C_6H_5 , ortho), 128.6 (C_6H_5 , meta), 126.7 (C_6H_5 , para); $\text{Fe}(\text{CO})_3(1,4\text{-diphenylbutadiene})$ 60.7 (C-1 and C-4), 79.4 (C-2 and C-3), 139.7 (C_6H_5), 128.7 (C_6H_5 , ortho), 126.3 (C_6H_5 , meta), 126.7 (C_6H_5 , para), 211.3 (CO).

Raman, IR, and ESR Spectral Measurements. Raman spectra were run on a JASCO R-800 spectrometer with 514.5-nm (100 mW) argon ion laser as well as 63.3-nm (50 mW) He-Ne ion laser excitations at 30 °C. The doped or undoped powdered samples are placed in Pyrex tube under an argon atmosphere. Infrared spectra were obtained on a JASCO DS-402G spectrometer. The samples were used in a form of KBr disks. EPR spectra were carried out on a JEOL Fe-1X spectrometer with 100-kHz field modulation in the temperature range 4–320 K by utilizing Mn^{2+} in MgO as a standard.

Cyclic voltammetry at potential scan rates faster than 0.3 V/s was carried out in Ar on a Yanaco P8-CV at 25 °C with a three-electrode system consisting of a glassy carbon working electrode, a platinum wire auxiliary electrode, and a saturated calomel electrode as the reference. Samples were dissolved in DMF (2 mM), and $[\text{N}(n\text{-Bu})_4][\text{ClO}_4]$ was used as a supporting electrolyte.

Powder X-ray diffraction data and spectra are given in Figures 7–9 for 1.

Acknowledgment. We thank Dr. W. Mori of Faculty of Education, Osaka University, for the computer analysis of the powder X-ray diffractions.